Carcinogenesis vol.30 no.8 pp.1416–1423, 2009
doi:10.1093/carcin/bgp147
Advance Access publication June 15, 2009

α-Keto acid metabolites of organoselenium compounds inhibit histone deacetylase activity in human colon cancer cells

Hui Nian[1,2], William H.Bisson[2], Wan-Mohaiza Dashwood[2], John T.Pinto[3] and Roderick H.Dashwood[2,4,*]

[1]Department of Biochemistry and Biophysics and [2]Linus Pauling Institute, Oregon State University, Corvallis, OR 97331, USA, [3]Department of Biochemistry and Molecular Biology, New York Medical College, Valhalla, NY 10595, USA and [4]Department of Environmental and Molecular Toxicology, Oregon State University, Corvallis, OR 97331, USA

[*]To whom correspondence should be addressed. Tel: +1 541 737 5086; Fax: +1 541 737 5077;
Email: rod.dashwood@oregonstate.edu

Methylselenocysteine (MSC) and selenomethionine (SM) are two organoselenium compounds receiving interest for their potential anticancer properties. These compounds can be converted to β-methylselenopyruvate (MSP) and α-keto-γ-methylselenobutyrate (KMSB), α-keto acid metabolites that share structural features with the histone deacetylase (HDAC) inhibitor butyrate. We tested the organoselenium compounds in an *in vitro* assay with human HDAC1 and HDAC8; whereas SM and MSC had little or no activity up to 2 mM, MSP and KMSB caused dose-dependent inhibition of HDAC activity. Subsequent experiments identified MSP as a competitive inhibitor of HDAC8, and computational modeling supported a mechanism involving reversible interaction with the active site zinc atom. In human colon cancer cells, acetylated histone H3 levels were increased during the period 0.5–48 h after treatment with MSP and KMSB, and there was dose-dependent inhibition of HDAC activity. The proportion of cells occupying G_2/M of the cell cycle was increased at 10–50 μM MSP and KMSB, and apoptosis was induced, as evidenced by morphological changes, Annexin V staining and increased cleaved caspase-3, -6, -7, -9 and poly(adenosine diphosphate-ribose)polymerase. *P21WAF1*, a well-established target gene of clinically used HDAC inhibitors, was increased in MSP- and KMSB-treated colon cancer cells at both the messenger RNA and protein level, and there was enhanced *P21WAF1* promoter activity. These studies confirm that in addition to targeting redox-sensitive signaling molecules, α-keto acid metabolites of organoselenium compounds alter HDAC activity and histone acetylation status in colon cancer cells, as recently observed in human prostate cancer cells.

Introduction

Methylselenocysteine (MSC) and selenomethionine (SM) are two major organoselenium compounds present in selenium-enriched plants and yeast (1). Both of these compounds have reported anticancer properties, including in breast, prostate and colon cancer cells (2–8). For example, in mouse mammary epithelial tumor cells *in vitro*, MSC attenuated phosphatidylinositol 3-kinase activity, reduced the phosphorylation of p38 and inhibited the Raf–mitogen-activated protein kinase–extracellular regulated kinase-signaling pathway (3). In human colon cancer cells, SM regulated cyclooxygenase-2 expression via nuclear factor-kappaB, and apoptosis induction was p53 dependent and mediated by superoxide (5,6). It has been suggested that methylselenol (MS), a β- or γ-elimination product of MSC and SM, may be a key metabolite for cancer chemoprevention, acting to redox-modify proteins and regulate key signaling pathways (9). However, MS may not be the only metabolite with important biological activity. In the liver, MSC and SM undergo transamination reactions to generate β-methylselenopyruvate (MSP) and α-keto-γ-methylselenobutyrate (KMSB), respectively (Figure 1). The widely distributed enzyme glutamine transaminase K also efficiently converts MSC to MS and MSP (10).

MSP and KMSB share structural features with butyrate, a short-chain fatty acid reported to competitively inhibit histone deacetylase (HDAC) activity (11). HDAC inhibitors have received increasing interest as cancer therapeutic agents, due to their potential to de-repress epigenetically silenced genes via changes in histone acetylation status (12–16). Interestingly, the human diet contains several chemopreventive agents that also inhibit HDAC activity, helping to trigger cell cycle arrest/apoptosis in cancer cells through chromatin remodeling (17–24). We reported previously on the HDAC inhibitory effects of sulforaphane from broccoli and garlic-derived organosulfur compounds (22–24). The search continues for novel dietary agents that might be used alone or in combination with HDAC inhibitor drugs being developed as candidates for cancer therapy (12–16). There is also interest in learning, from a basic mechanistic standpoint, how different dietary agents influence HDAC activity, histone acetylation status and the expression of cell cycle regulators, such as $p21^{WAF1}$ (p21). In this report, we describe for the first time the HDAC inhibitory effects of organoselenium compounds in human colon cancer cells and the corresponding changes in cell growth, apoptosis and p21 expression.

Abbreviations: HDAC, histone deacetylase; KMSB, α-keto-γ-methylselenobutyrate; mRNA, messenger RNA; MS, methylselenol; MSC, methylselenocysteine; MSP, β-methylselenopyruvate; PBS, phosphate-buffered saline; SM, selenomethionine; TUNEL, terminal deoxynucleotidyl transferase deoxyuridine triphosphate nick end labeling.

Material and methods

Cell culture and reagents

Human HT29 and HCT116 colon cancer cell lines were obtained from American Type Culture Collection (Manassas, VA) and cultivated in McCoy's 5A medium (Life Technologies, Carlsbad, CA) supplemented with 1% penicillin–streptomycin and 10% fetal bovine serum. In some experiments, HCT116 ($p53^{-/-}$) and HCT116 ($p53^{+/+}$) cells were used, kindly provided by Dr Bert Vogelstein (Johns Hopkins University, Baltimore, MD). MSC, SM, MSP and KMSB were generated as reported elsewhere (10).

HDAC activity

HDAC activity was determined using the Fluor-de-Lys HDAC activity assay kit (Biomol, Plymouth Meeting, PA), as reported before (24). Incubations were performed at 37°C with purified human HDAC8, human HDAC1 or nuclear extracts from colon cancer cells. Fluorescence was measured using a Spectra MaxGemini XS fluorescence plate reader (Molecular Devices, Sunnyvale, CA), with excitation at 360 nm and emission at 460 nm.

Molecular docking

Coordinates of the human HDAC8 catalytic domain were taken from the crystal structures available in the Protein Data Bank 1T67 (MS-344/HDAC-8) (25). The model was energetically refined in the internal coordinate space with Molsoft ICM v3.5-1p (26). The docking was represented by five types of interaction potentials: (i) van der Waals potential for a hydrogen atom probe; (ii) van der Waals potential for a heavy-atom probe (generic carbon with 1.7 Å radius); (iii) optimized electrostatic term; (iv) hydrophobic terms and (v) loan-pair-based potential, which reflects directional preferences in hydrogen bonding. The energy terms were based on the all-atom vacuum force field ECEPP/3 with appended terms from the Merck Molecular Force Field to account for solvation free energy and entropic contribution. Modified intermolecular terms such as soft van der Waals and hydrogen bonding as well as a hydrophobic term were included. Conformational sampling was based on the biased probability Monte Carlo procedure, with full local minimization after each randomization step. In the ICM-VLS (Molsoft ICM v3.5-1p) screening procedure, ligand scoring was optimized to obtain maximal separation between bound and unbound species. Each selenium compound was assigned a score according to fit within the pocket, accounting for electrostatic, hydrophobic and entropy parameters (27).

Dimethyl thiazolium bromide assay

Cell growth was determined by assaying for the reduction of dimethyl thiazolium bromide to formazan. Briefly, after 48 h incubation with MSP or KMSB,

10 μl dimethyl thiazolium bromide (5 μg/μl) was added to cells in 96-well plates. Cells were incubated at 37°C for 4 h, and a Spectra MaxGemini XS fluorescence plate reader (Molecular Devices) was used to measure absorbance at 620 nm for each well. Growth rate was calculated as follows: Cell growth = (A_{620} treated cells/A_{620} control cells) × 100%.

Flow cytometry

Cells treated with MSP or KMSB for 8 and 24 h were harvested in cold phosphate-buffered saline (PBS), fixed in 70% ethanol and stored at 4°C for at least 48 h. Fixed cells were washed with PBS once and resuspended in propidium iodide/Triton X-100 staining solution containing RNase A. Samples were incubated in the dark for 30 min before cell cycle analysis. The DNA content of the cells was detected using EPICS XL Beckman Coulter and analyses of cell distribution in the different cell cycle phases were performed using Multicycle Software (Phoenix Flow Systems, San Diego, CA).

TUNEL assay

Terminal deoxynucleotidyl transferase deoxyuridine triphosphate nick end labeling (TUNEL) was performed using a Guava TUNEL kit (Guava Technologies, Hayward, CA), in accordance with the manufacturer's protocol. Briefly, cells were treated with 0–50 μM MSP or KMSB for 48 h and then fixed with 1% paraformaldehyde on ice for 1 h. After washing with PBS twice, 70% ethanol was added to the cell pellet and incubated at −20°C to permeabilize the cells for 24 h. The cells were washed with Wash Buffer twice and incubated in the DNA-labeling Solution (including terminal deoxynucleotidyl transferase enzyme and BrdU-uridine triphosphate) for 60 min at 37°C in a water bath. Cells were rinsed and collected by centrifugation and incubated in anti-BrdU-staining mix for 45 min at room temperature. Data were acquired on a Guava PCA instrument.

Annexin V assay

Annexin V staining was performed using the Guava Nexin kit (Hayward, CA), in accordance with the manufacturer's protocol. Briefly, cells were treated with 0–50 μM MSP or KMSB for 24 h and collected by centrifugation. After washing with PBS, the cells were incubated in Nexin buffer containing Annexin V and 7-AAD on ice for 20 min. Data were acquired on a Guava PCA instrument.

Immunoblotting

Protein concentration of cell lysates was determined using the bicinchoninic acid assay (Pierce, Rockford, IL). Proteins (20 mg) were separated by sodium dodecyl sulfate–polyacrylamide gel electrophoresis on 4–12% Bis-Tris gel (Novex, San Diego, CA) and transferred to nitrocellulose membranes (Invitrogen, Carlsbad, CA). Membranes were saturated with 2% bovine serum albumin

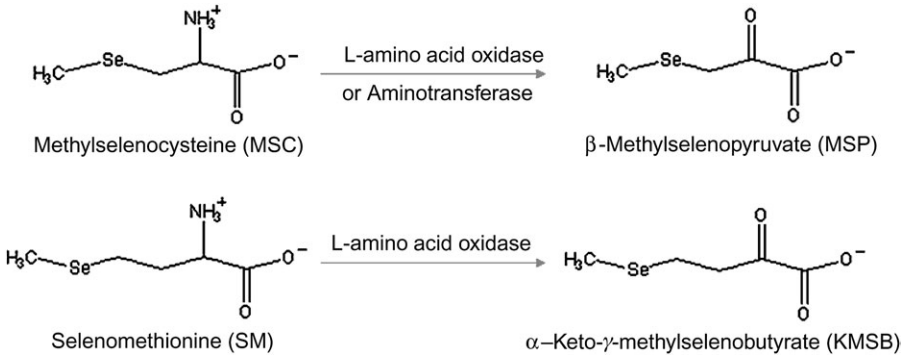

Fig. 1. Deamination reactions of organoselenium compounds MSC and SM to generate α-keto acid metabolites, MSP and KMSB, respectively.

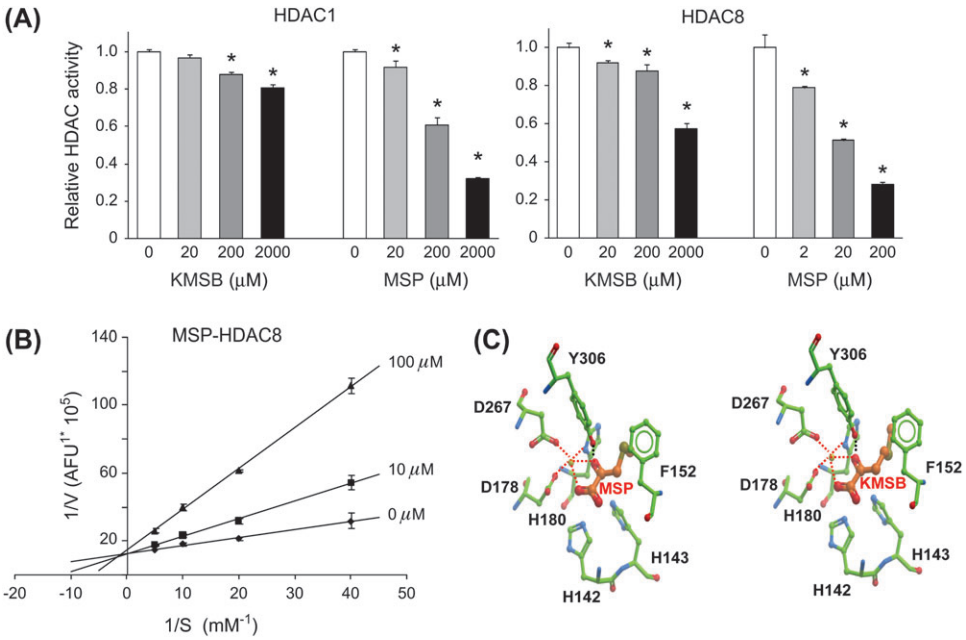

Fig. 2. KMSB and MSP inhibit HDAC activity. (**A**) HDAC assays were performed with purified human HDAC1 and HDAC8, in the presence of different concentrations of MSP or KMSB. Data = mean ± SD, $n = 3$, $^*P < 0.05$. (**B**) Kinetics of HDAC8 inhibition by MSP. Reaction velocities were measured at different concentrations of substrate, in the presence of 0, 10 and 100 μM MSP. The Lineweaver-Burk plot indicated competitive inhibition (K_i = 35 μM). (**C**) Docking of MSP (left) and KMSB (right) into human HDAC8 catalytic domain (ICM v3.5-1p). Zinc coordination is represented by red dashed lines. H-bonds are represented by black dashed lines between donor and acceptor atoms, defined as follows: Distance D—A: 2.8–3.2 Å; Angle D-H—A: 140–180°.

for 1 h, followed by overnight incubation at 4°C with primary antibodies against acetylated histone H3 (1:200, Upstate, Temecula, CA, #06-599), histone H3 (1:200, Upstate, #06-755), p21 (1:1000, Cell Signaling, Beverly, MA, #2947) or β-actin (A5441, 1:5000, Sigma, Saint Louis, MO). Membranes were then incubated with peroxidase-conjugated secondary antibodies (Bio-Rad, Hercules, CA) for 1 h. Immunoreactive bands were visualized by using Western Lightning Chemiluminescence Reagent Plus (PE Life Sciences, Boston, MA) and detected with an AlphaInnotech imaging system.

Reverse transcription–polymerase chain reaction and quantitative real-time polymerase chain reaction

Cells treated with MSP or KMSB were disrupted by using QIAshredder spin column (QIAGEN, Santa Clarita, CA) and total RNA was extracted using the RNeasy® Mini kit (QIAGEN) in accordance with the manufacturer's instructions. Single-strand complementary DNA was then synthesized with 5 μg of total RNA using the High-Capacity complementary DNA Archive kit (Applied Biosystems, Foster city, CA), according to the manufacturer's protocol. Real-time amplification was achieved using an ABI Prism 7500 Real-Time PCR instrument (Applied Biosystems). Pairs of primers and TaqMan probes were obtained from Applied Biosystems (TaqMan® Gene Expression Assays). Polymerase chain reaction was performed as follows: denaturation for 10 min at 95°C, followed by 50 cycles at 95°C for 15 s and 60°C for 1 min. The linear range of amplification was determined using serially diluted complementary DNA (4-fold series). The messenger RNA (mRNA) expression of the target gene was normalized to the corresponding *GAPDH* internal control.

Luciferase assay

The effects of MSP and KMSB on *P21WAF1* promoter activity were determined by dual luciferase reporter gene assay. The full-length 5′-regulatory region (p21P) and the deletion mutants p21PΔ1.1, p21Psma and p21PsmaΔ1 containing firefly luciferase gene were gifts of Dr Xiao-Fan Wang (28). pRL-CMV plasmid containing the renilla luciferase gene (Promega, Madison, WI) was used as internal control. HT29 cells were cultured in 60 mm plates for 24 h. Plasmid construct (4 μg), 10 ng pRL-CMV plasmid DNA and 12 ml TransFast reagent (Promega, Madison, WI) were mixed together in 2 ml media and used to transfect each plate in the absence of serum. After 1 h, 4 ml 10% serum media

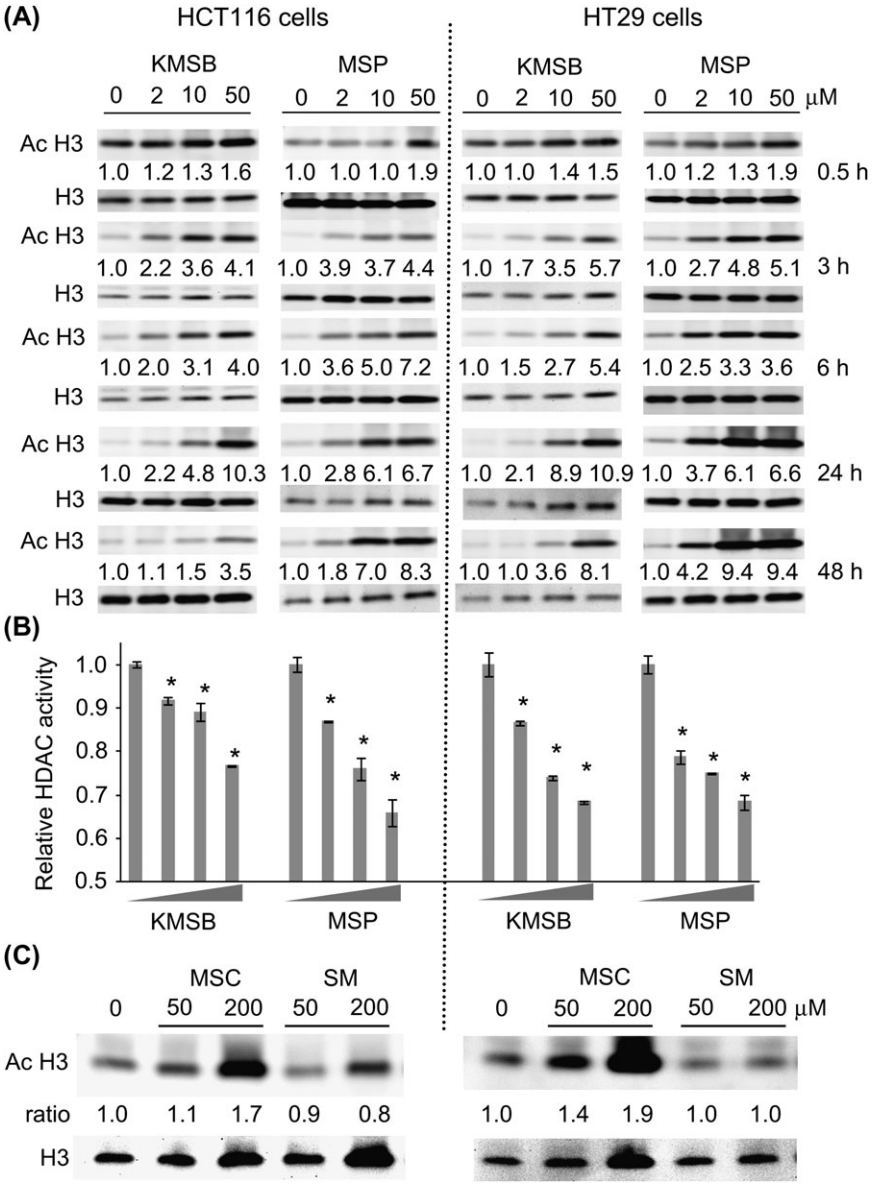

Fig. 3. Histone acetylation induced by KMSB and MSP in human colon cancer cells. (**A**) HT29 and HCT116 cells were exposed to 0, 2, 10 and 50 μM KMSB or MSP, and at the times shown, acetylated histone H3 (Ac H3) levels were assessed by immunoblotting. Total histone H3 (H3) expression was used as reference control. The ratio of Ac H3:H3 expression is shown for each lane, with the 0 μM treatment control assigned an arbitrary value of 1.0. (**B**) HDAC activities in nuclear extracts of HCT116 and HT29 cells 3 h after treatment with 0, 2, 10 and 50 μM KMSB or MSP (wedge symbol). Data = mean ± SD, $n = 3$, $^*P < 0.05$. (**C**) HCT116 and HT29 cells were exposed to 0, 50 or 200 μM MSC or SM (selenium parent compounds, see Figure 1), followed by immunoblotting for Ac H3 and H3 at 24 h.

containing MSP or KMSB were added to the plates. Twenty-four hours later, cells were lysed and luciferase assays were performed using the Dual Luciferase Reporter Assay System (Promega). The relative luciferase activity reported here is the ratio of firefly luciferase activity over renilla luciferase activity.

Chromatin immunoprecipitation

Chromatin immunoprecipitation assays were performed based on a published methodology (24). In brief, HT29 cells were cultured with 10 μM MSP for 4 h and fixed in 1% formaldehyde for 10 min at room temperature. Cross-linking was stopped by adding glycine at a final concentration of 0.125 M. The chromatin immunoprecipitation kit from Active Motif (Carlsbad, CA) was used according to the manufacturer's instructions. Chromatin was incubated with anti-RNA polymerase II antibody (provided with the kit), anti-histone H3 (Cell Signaling, #2650, 1:50), anti-acetylated histone H3-Lys9 (Cell Signaling, #9671, 1:50) and anti-acetylated histone H3-Lys18 (Cell Signaling, #9675, 1:25). The corresponding blocking peptide was used to confirm antibody specificity [i.e. acetyl-histone H3 (Lys 9)-blocking peptide (Cell Signaling, #1083, 1:500) and acetyl-histone H3 (Lys 18)-blocking peptide (Abcam, Cambridge, MA, #24003, 1:1000), data not shown]. DNA pull down was purified by phenol–chloroform extraction followed by ethanol precipitation. Data were quantified with a LightCycler 480 II (Roche, Indianapolis, IN) for *P21WAF1* gene promoter region −249 to −389, using primers F 5′-GTAAATCCTTGCCTGCCAGA-3′ and R 5′-ACATTTCCCCACGAAGTGAG-3′. Polymerase chain reaction conditions were 15 s at 95°C, 10 s at 60°C and 10 s at 72°C.

Statistics

Where indicated, results were expressed as mean ± SD. Statistical significance was evaluated for data from three independent experiments using Student's *t*-test. A *P*-value <0.05 was considered to be statistically significant and indicated as such with an asterisk (*) on the corresponding figures. Statistical analyses were performed by Dr Clifford B.Pereira, Department of Statistics, Oregon State University.

Results

MSP and KMSB inhibit HDAC activity

We first studied the HDAC inhibitory effects of MSP and KMSB using purified human HDAC1 and HDAC8 enzymes in a cell-free system (Figure 2A). Both α-keto acids inhibited HDAC activity in a dose-dependent manner with MSP being especially effective against HDAC8 (IC_{50} ∼20 μM). Under the same experimental conditions, the parent compounds MSC and SM had little or no effect on HDAC activity (data not presented). Thus, the inhibitory potency toward HDAC8 was in the order: MSP>KMSB>>MSC>SM. By varying the concentrations of substrate and test agent, we examined the kinetics of HDAC8 inhibition by MSP. In the Lineweaver-Burk plot, lines of increasing slope intersected on the *y*-axis (Figure 2B); thus, MSP was identified as a competitive inhibitor, with the potential to bind reversibly to the HDAC8 active site. Based on the available crystal structure with bound inhibitors (25,29), we simulated the possible interaction between MSP and HDAC8. Molecular modeling indicated that MSP docked in an energetically favored orientation, with the α-carbonyl group and one of the carboxylate oxygen atoms coordinating with the buried zinc (Figure 2C, left). KMSB adopted a similar orientation in the HDAC8 active site using the iterative docking procedure (Figure 2C, right).

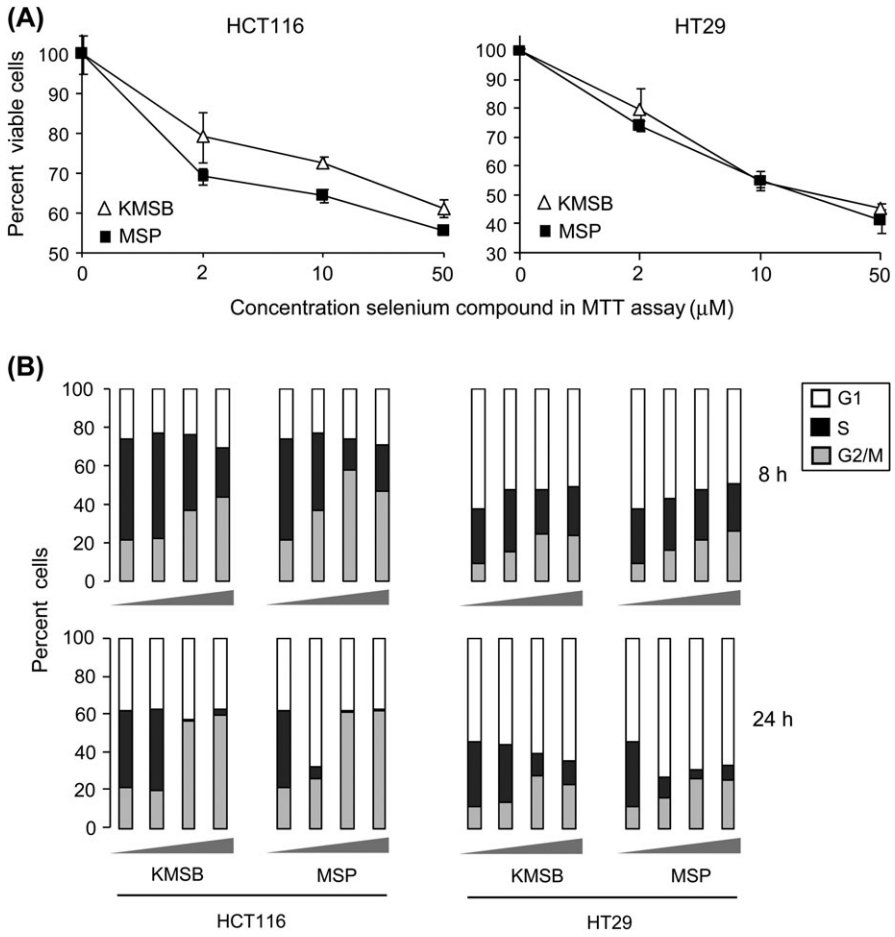

Fig. 4. KMSB and MSP suppress cell growth and induce cell cycle arrest. (**A**) In the dimethyl thiazolium bromide (MTT) assay, HCT116 and HT29 cells treated with 0, 2, 10 and 50 μM KMSB or MSP displayed dose-dependent loss of cell viability at 48 h. Data = mean ± SD, $n = 3$. (**B**) HCT116 and HT29 cells were exposed to 0, 2, 10 and 50 μM KMSB or MSP (wedge symbol). The percentage of cells occupying G_1, S and G_2/M phases of the cell cycle was determined by flow cytometry. Results are shown for cells collected 8 and 24 h after treatment and are representative of three independent experiments.

MSP and KMSB increase histone acetylation in human colon cancer cells

HCT116 and HT29 human colon cancer cells were used to investigate the cellular effects of MSP and KMSB. Cells were exposed to 2, 10 and 50 μM KMSB or MSP for selected times, and the levels of global histone H3 acetylation were examined by immunoblotting of whole-cell lysates (Figure 3A). Dose-dependent increases in acetylated histone H3 were detected as early as 30 min after MSP and KMSB treatment, which persisted for at least 48 h. For example, in HT29 cells treated with 2, 10 and 50 μM MSP (Figure 3A, right), acetylated histone H3 levels were increased 1.2-, 1.3- and 1.9-fold at 0.5 h and 4.2-, 9.4- and 9.4-fold at 48 h, compared with 0 μM MSP. At the highest concentration of 50 μM MSP and KMSB, HDAC inhibition was evident in nuclear extracts at 30 min (data not shown), and dose-dependent loss of HDAC activity was detected by 3 h (Figure 3B). MSC and SM parent compounds, however, had no effect on histone H3 acetylation or HDAC activity up to 5 h after treatment (data not shown). By 24 h, MSC at the highest concentration tested (200 μM) increased histone H3 acetylation in both cell lines, whereas SM had no effect after normalizing to total histone H3 levels in the whole-cell lysates (Figure 3C).

MSP and KMSB inhibit cell growth and induce cell cycle arrest/apoptosis

In human colon cancer cells, treatment with MSP or KMSB resulted in dose-dependent loss of cell viability. For example, 48 h after exposure to 50 μM MSP or KMSB, ~60% of HCT116 cells and ~40% of HT29 cells remained viable (Figure 4A). The two highest concentrations of 10 and 50 μM MSP and KMSB increased the proportion of cells occupying the G_2 phase of the cell cycle, most notably in HCT116 cells at 8 and 24 h (Figure 4B). At 24 h, the lowest concentration of 2 μM MSP increased the proportion of cells in G_1 and decreased the proportion in S phase, but this was not evident for 2 μM KMSB. We recently reported similar findings for trichostatin A, such that arrest in G_1 versus G_2 of the cell cycle was dependent on the dose of the HDAC inhibitor (24).

Colon cancer cells treated with MSP or KMSB developed a rounded morphology and detached from the plate, indicative of apoptosis (data not shown). In the Annexin V assay, there was a dose-dependent increase in positively labeled cells after treatment with MSP or KMSB (Figure 5A). At the highest concentration of MSP and KMSB (50 μM), >50% HCT116 cells and 20% HT29 cells were Annexin positive, compared with ~7% for the controls. In the TUNEL assay, there was evidence for increased DNA fragmentation (Figure 5B). For example, 48 h after treatment with 50 μM MSP or KMSB, >50% HCT116 cells and 20% HT29 cells were TUNEL positive. Caspase activation also was examined by immunoblotting (Figure 5C). Cleaved caspases -3, -6, -7 and -9, as well as cleaved poly ADP ribose polymerase, were increased in a dose-dependent manner 24 h after treatment with MSP or KMSB. No corresponding changes were detected for cleaved caspase-8 (data not shown).

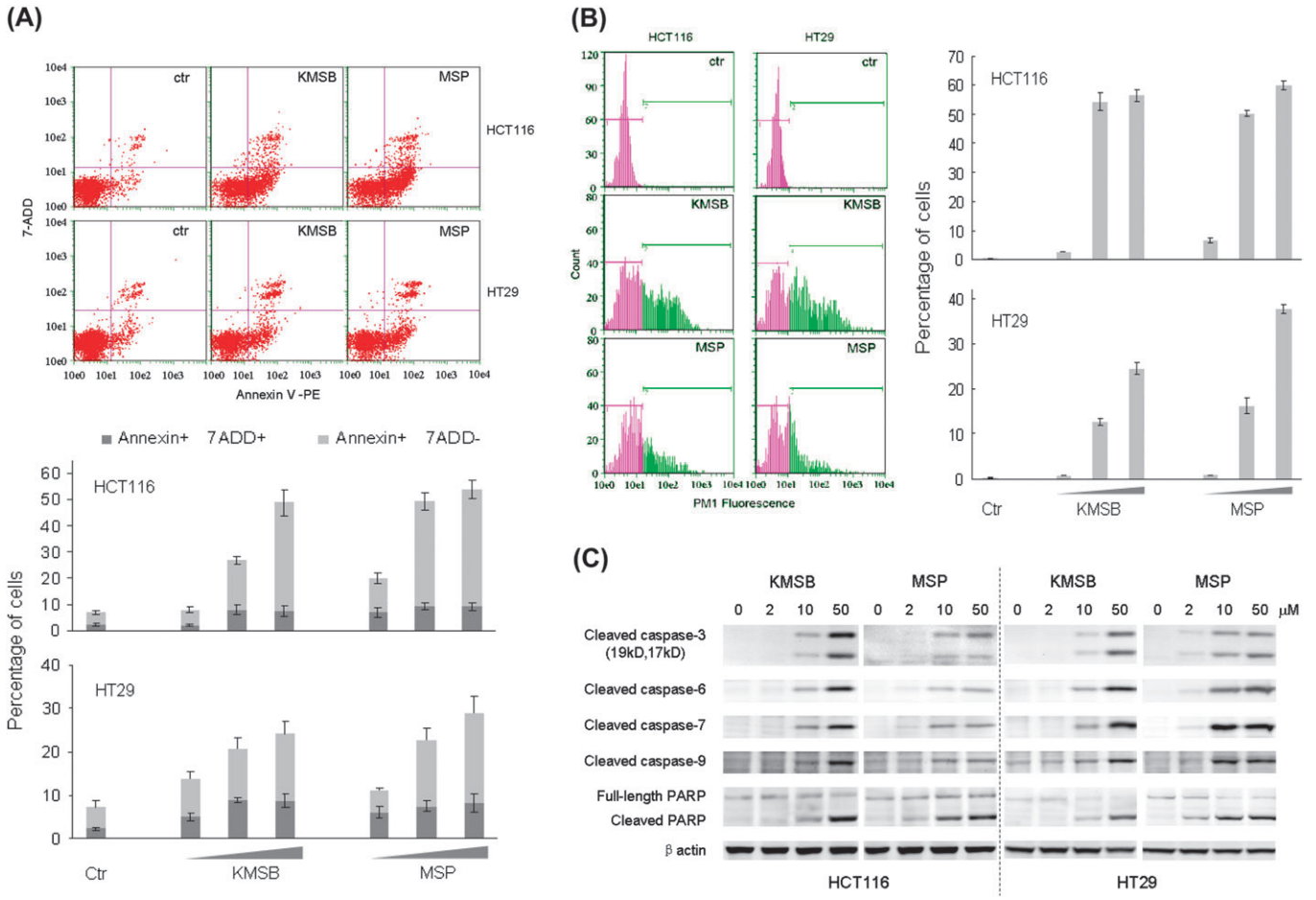

Fig. 5. KMSB and MSP induce apoptosis in colon cancer cells. (**A**) HCT116 and HT29 cells were exposed to 2, 10 and 50 μM KMSB or MSP (wedge symbol) or vehicle alone (control, Ctr). Cells were stained 24 h later with Annexin V-PE and 7-AAD (top). Annexin V (+) and 7-AAD (−) indicates early apoptotic cells, whereas Annexin v (+) and 7-AAD (+) indicates late-stage apoptotic cells. The percentage of cells in each population is summarized as mean ± SD, $n = 3$ (bottom). (**B**) Cells were fixed 48 h after treatment with 2, 10 and 50 μM KMSB or MSP (wedge symbol) or vehicle alone (control, Ctr), and TUNEL-positive cells were quantified, see Materials and Methods. Data bars = mean ± SD, $n = 3$ (right). (**C**) Cells were treated with KMSB or MSP and immunoblotted 24 h later for cleaved caspase-3 (two cleaved products of 19 and 17 kDa), -6, -7, -9 and poly ADP ribose polymerase (full-length and cleaved bands). β-Actin, loading control.

MSP and KMSB induce p21

The cell cycle regulator p21 is a well-established target of HDAC inhibitor drugs (16,30) and dietary HDAC inhibitors (21–23). HT29 cells have low endogenous levels of p21, but p21 protein expression was elevated for at least 24 h after MSP or KMSB treatment (Figure 6A). Quantitative reverse transcription–polymerase chain reaction analyses revealed that MSP and KMSB also increased *p21* mRNA levels in HT29 cells (Figure 6B). For example, 2, 10 and 50 μM concentrations of KMSB increased *p21* mRNA expression 1.5-, 6- and 13-fold, respectively.

Chromatin immunoprecipitation assays of the *P21WAF1* promoter revealed a slight decrease in Pol II and histone H3 levels and a 2- to 3-fold increase in acetylated histone H3 K9 and acetylated histone H3 K18 levels, 4 h after HT29 cells were treated with 10 μM MSP (Figure 6C). No significant changes were detected for the promoter region of a control gene (*ACTB*) under the same experimental conditions (data not presented).

In HT29 cells transfected with a *P21WAF1* promoter–reporter containing p53 and Sp1/Sp3 sites, 10 μM MSP or KMSB increased the luciferase activity significantly (Figure 6D). Deletion of the p53 and Sp1/Sp3 sites decreased the basal reporter activity (compare white bars in Figure 6D), but as long as the Sp1/Sp3 sites were present, MSP and KMSB both increased the reporter activity compared with the corresponding control. Deletion of the Sp1/Sp3 sites (in p21PSmaΔ1) completely abrogated the response to MSP and KMSB.

To examine the role of p53, HCT116 ($p53^{-/-}$) and HCT116 ($p53^{+/+}$) cells were treated with 10 μM MSP and 12 h later, the whole-cell lysates were immunoblotted for p53, p21 and acetylated histone H3 (Figure 6E). As expected, p53 was detected in HCT116 ($p53^{+/+}$) but not in HCT116 ($p53^{-/-}$) cells, and MSP had no effect on the basal p53 expression in either cell line. Higher levels of endogenous p21 were detected in HCT116 ($p53^{+/+}$) than HCT116 ($p53^{-/-}$) cells, but in both cell lines MSP strongly induced p21 as well as acetylated histone H3. Histone H3 and β-actin, which served as loading controls, were unaffected by MSP treatment.

Discussion

We report here, for the first time, that MSP and KMSB inhibited human HDAC1 and HDAC8 activities in a concentration-dependent manner *in vitro*. Enzyme kinetics studies coupled with molecular modeling supported a mechanism involving reversible competitive

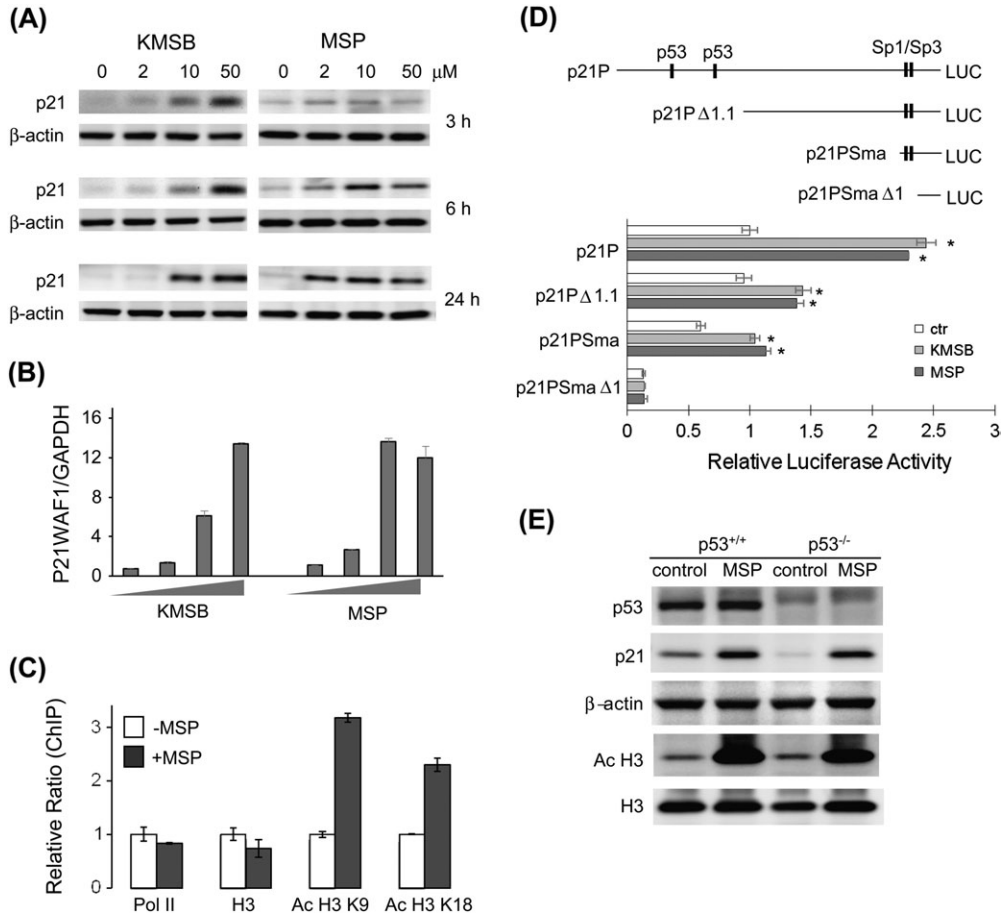

Fig. 6. Induction of p21 by KMSB and MSP. (**A**) HT29 cells were exposed to 0, 2, 10 and 50 μM KMSB or MSP, and 3, 6 or 24 h later, p21 expression was determined by immunoblotting. (**B**) Quantitative reverse transcription–polymerase chain reaction data for *p21* mRNA expression (normalized to *GAPDH*), 6 h after HT29 cells were treated with 0, 2, 10 and 50 μM KMSB or MSP (wedge symbol). Data bars = mean ± SD, $n = 3$. (**C**) Chromatin immunoprecipitation (ChIP) assays of the *P21WAF1* promoter were performed 4 h after treatment with 10 μM MSP, using the indicated antibodies, and output was quantified by quantitative polymerase chain reaction and normalized to input (relative ratio). Data = mean ± SD, $n = 3$, from a single experiment and are representative of findings from three independent experiments. (**D**) HT29 cells were treated with 10 μM KMSB or MSP, and 24 h later, *p21* transcriptional activity was determined using a luciferase (LUC) reporter, as described in Materials and Methods. Results are expressed as relative luciferase activity, mean ± SD, $n = 3$; $^*P < 0.05$ versus control (Ctr). Upper diagram illustrates constructs that contained full-length 5′-regulatory region harboring both p53 and Sp1/Sp3 sites (p21P), deletion of p53 sites (p21PΔ1.1) or the minimal promoter with (p21PSma) or without (p21PSmaΔ1) Sp1/3 sites. (**E**) HCT116 ($p53^{+/+}$) and HCT116 ($p53^{-/-}$) cells were treated with 10 μM MSP, and 12 h later, the whole-cell lysates were immunoblotted for p53, p21 and acetylated histone H3 (Ac H3), with histone H3 and β-actin as loading controls. Data are representative of the findings from two separate experiments.

inhibition, as seen for other small molecule inhibitors, such as butyrate and allyl mercaptan (11,24). The predicted orientation of MSP and KMSB in the HDAC pocket resembled that of known HDAC inhibitor drugs, which coordinate with the zinc atom and establish H-bond partners with buried polar residues. Considering the conserved nature of the HDAC active site, it is probable that MSP and KMSB will inhibit other class I and class II HDACs by competing with substrate for binding to the enzyme. An important distinction, however, is that nM K_i values are typical for the more potent HDAC inhibitors used in the clinical setting, whereas butyrate, allyl mercaptan and MSP have inhibitor constants on the order 46, 24 and 35 μM, respectively (refs 11,24 and this study). As discussed elsewhere (24,31), dietary HDAC inhibitors typically produce a more sustained level of histone hyperacetylation with lower toxicity than HDAC inhibitor drugs. Thus, dietary isothiocyanates, organosulfur compounds and organoselenium metabolites might be combined with lower doses of clinically used HDAC inhibitors to minimize toxicity and augment the therapeutic efficacy.

Colon cancer cells treated with MSP or KMSB had increased levels of p21 mRNA and protein expression, and there was increased histone acetylation associated with the *P21WAF1* promoter region. Previous studies implicated p21 as a downstream target of HDAC inhibitor drugs (16,30). We have reported that dietary HDAC inhibitors, such as sulforaphane and allyl mercaptan, increase p21 mRNA and protein expression in human cancer cells, with evidence for histone hyperacetylation on the *P21WAF1* promoter and enhanced binding of the transcription factor Sp3 (22–24). Consistent with the latter findings, MSP and KMSB increased the activity of a *P21WAF1* luciferase reporter in HT29 cells, except when the Sp1/Sp3 sites were eliminated, and p21 mRNA and protein levels were elevated markedly. Deletion of the p53-binding sites did not interfere with the ability of KMSB or MSP to induce *P21WAF1* reporter activity. We also observed that in p53-null HCT116 ($p53^{-/-}$) cells, MSP strongly increased the expression of acetylated histone H3, as well as p21 (Figure 6E). These findings suggest that the mechanism of p21 induction is probably p53 independent, although in cells that contain p53 (wild-type or mutant) there may be a role for p53 at later time points, as reported for allyl mercaptan (24). In addition to p21, we are interested in studying other potential targets, and several interesting candidates have been implicated in prior studies with HDAC inhibitor drugs (32–34). Given the level of apoptosis induction in response to MSP and KMSB treatment (Figure 5), bax and related Bcl-2 family members may be worthy of investigation (22).

Much interest of late has focused on the anticancer effects of selenium-enriched yeast and SM. However, selenium-enriched broccoli florets and broccoli sprouts containing high levels of MSC inhibited colon tumor development in several preclinical studies (35–37). Interestingly, SM produced negative or equivocal results in colon cancer models (38–40), and addition of inorganic selenite to regular broccoli florets or broccoli sprout powder proved ineffective for the reduction of colon tumors. In a side-by-side comparison, selenium-enriched garlic was more than twice as effective as selenium-enriched yeast for mammary cancer chemoprevention (41). Collectively, these studies clearly indicate that the chemical form of selenium impacts significantly on the potential for cancer chemoprevention.

It has been suggested that MS may be a key active metabolite of MSC, SM and other selenocompounds (9). The working hypothesis is that MS can redox-modify cysteine-rich regions in proteins, altering their conformation and activity, thereby regulating signaling pathways and gene expression (42). Protein kinase C has been postulated as a direct target for redox modification by MS (43). The variation in chemopreventive efficacy between different selenocompounds was presumed to be associated with their different abilities to generate MS. However, this may not be the entire story. MSC is a good substrate for glutamine transaminase K, an enzyme that is widely distributed in mammalian tissues, but which has low activity toward SM (44). We observed histone hyperacetylation after 24 h in colon cancer cells treated with 200 μM MSC, but not SM, and at 5 h, no change in histone acetylation status was detected for either compound. Also, in experiments with the *P21WAF1* promoter–reporter, MSC increased the transcriptional activity after 24 h, whereas SM had no effect (data not shown). We interpret these findings as indirect evidence for the conversion of MSC, but not SM, to the α-keto acid metabolite in human colon cancer cells. Support for this idea comes from experiments in human prostate cancer cells, which contain endogenous glutamine transaminase K and convert MSC, but not SM, to the α-keto acid metabolite (45). Given the disappointing news from the selenium and Vitamin E Cancer Prevention Trial, in which selenium supplements were provided as SM (46), we believe it is now timely to consider a new chemoprevention paradigm for organoselenium compounds. Specifically, MSC and other organoselenium compounds might generate α-keto acid metabolites as HDAC inhibitors, with the potential to affect histone status and chromatin remodeling, leading to derepression of silenced tumor suppressor genes.

Funding

National Institutes of Health (CA090890, CA065525, CA122959, CA111842); National Institute of Environmental Health Sciences center (P30 ES00210).

Acknowledgements

We thank Dr Xiao-Fan Wang (Department of Pharmacology, Duke University Medical Center, Durham, NC) for providing *P21WAF1* reporter constructs, Dr Bert Vogelstein (Johns Hopkins University, Baltimore, MD) for the generous gift of HCT116 ($p53^{-/-}$) and HCT116 ($p53^{+/+}$) cells, and Dr Clifford Pereira (Department of Statistics, and Integrated Health Sciences Core facility, Environmental Health Science Center, Oregon State University) for assistance with the statistical analyses.

Conflict of Interest Statement: None declared.

References

1. Gammelgaard,B. *et al*. (2008) Complementary use of molecular and element-specific mass spectrometry for identification of selenium compounds related to human selenium metabolism. *Anal. Bioanal. Chem.*, **390**, 1691–1706.
2. Ip,C. *et al*. (2000) Selenium modulation of cell proliferation and cell cycle biomarkers in normal and premalignant cells of the rat mammary gland. *Cancer Epidemiol. Biomarkers Prev.*, **9**, 49–54.
3. Unni,E. *et al*. (2005) Se-methylselenocysteine inhibits phosphatidylinositol 3-kinase activity of mouse mammary epithelial tumor cells *in vitro*. *Breast Cancer Res.*, **7**, R699–R707.
4. Sinha,R. *et al*. (1999) Effects of methylselenocysteine on PKC activity, cdk2 phosphorylation and gadd gene expression in synchronized mouse mammary epithelial tumor cells. *Cancer Lett.*, **146**, 135–145.
5. Zhao,R. *et al*. (2006) Apoptosis induced by selenomethionine and methioninase is superoxide mediated and p53 dependent in human prostate cancer cells. *Mol. Cancer Ther.*, **5**, 3275–3284.
6. Cherukuri,D.P. *et al*. (2005) Selenomethionine regulates cyclooxygenase-2 (COX-2) expression through nuclear factor-kappa B (NF-kappaB) in colon cancer cells. *Cancer Biol. Ther.*, **4**, 175–180.
7. Goel,A. *et al*. (2006) Selenomethionine induces p53 mediated cell cycle arrest and apoptosis in human colon cancer cells. *Cancer Biol. Ther.*, **5**, 529–535.
8. Goulet,A.C. *et al*. (2005) Selenomethionine induces sustained ERK phosphorylation leading to cell-cycle arrest in human colon cancer cells. *Carcinogenesis*, **26**, 109–117.
9. Ip,C. *et al*. (2002) New concepts in selenium chemoprevention. *Cancer Metastasis Rev.*, **21**, 281–289.
10. Cooper,A.J. *et al*. (2008) Substrate specificity of human glutamine transaminase K as an aminotransferase and as a cysteine S-conjugate beta-lyase. *Arch. Biochem. Biophys.*, **474**, 72–81.
11. Sekhavat,A. *et al*. (2007) Competitive inhibition of histone deacetylase activity by trichostatin A and butyrate. *Biochem. Cell Biol.*, **85**, 751–758.
12. Butler,L.M. *et al*. (2002) The histone deacetylase inhibitor SAHA arrests cancer cell growth, up-regulates thioredoxin-binding protein-2, and down-regulates thioredoxin. *Proc. Natl Acad. Sci. USA*, **99**, 11700–11705.
13. Glaser,K.B. *et al*. (2003) Gene expression profiling of multiple histone deacetylase (HDAC) inhibitors: defining a common gene set produced by

HDAC inhibition in T24 and MDA carcinoma cell lines. *Mol. Cancer Ther.*, **2**, 151–163.
14. Kumagai,T. *et al*. (2007) Histone deacetylase inhibitor, suberoylanilide hydroxamic acid (Vorinostat, SAHA) profoundly inhibits the growth of human pancreatic cancer cells. *Int. J. Cancer*, **121**, 656–665.
15. McLaughlin,F. *et al*. (2004) Histone deacetylase inhibitors open new doors in cancer therapy. *Biochem. Pharmacol.*, **68**, 1139–1144.
16. Okamoto,H. *et al*. (2006) Trichostatin A, an inhibitor of histone deacetylase, inhibits smooth muscle cell proliferation via induction of p21(WAF1). *J. Atheroscler. Thromb.*, **13**, 183–191.
17. Dashwood,R.H. *et al*. (2007) Dietary histone deacetylase inhibitors: from cells to mice to man. *Semin. Cancer Biol.*, **17**, 363–369.
18. Druesne,N. *et al*. (2004) Diallyl disulfide (DADS) increases histone acetylation and p21(waf1/cip1) expression in human colon tumor cell lines. *Carcinogenesis*, **25**, 1227–1236.
19. Lea,M.A. *et al*. (2001) Induction of histone acetylation in mouse erythroleukemia cells by some organosulfur compounds including allyl isothiocyanate. *Int. J. Cancer*, **92**, 784–789.
20. Lea,M.A. *et al*. (2002) Induction of histone acetylation and inhibition of growth of mouse erythroleukemia cells by S-allylmercaptocysteine. *Nutr. Cancer*, **43**, 90–102.
21. Myzak,M.C. *et al*. (2006) Histone deacetylases as targets for dietary cancer preventive agents: lessons learned with butyrate, diallyl disulfide, and sulforaphane. *Curr. Drug Targets*, **7**, 443–452.
22. Myzak,M.C. *et al*. (2006) Sulforaphane inhibits histone deacetylase *in vivo* and suppresses tumorigenesis in *Apc*^{min} mice. *FASEB J.*, **20**, 506–508.
23. Myzak,M.C. *et al*. (2004) A novel mechanism of chemoprotection by sulforaphane: inhibition of histone deacetylase. *Cancer Res.*, **64**, 5767–5774.
24. Nian,H. *et al*. (2008) Allyl mercaptan, a garlic-derived organosulfur compound, inhibits histone deacetylase and enhances Sp3 binding on the *P21WAF1* promoter. *Carcinogenesis*, **29**, 1816–1824.
25. Somoza,J.R. *et al*. (2004) Structural snapshots of human HDAC8 provide insights into the class I histone deacetylases. *Structure*, **12**, 1325–1334.
26. Cardozo,T. *et al*. (1995) Homology modeling by the ICM method. *Proteins*, **23**, 403–414.
27. Totrov,M. *et al*. (1997) Flexible protein-ligand docking by global energy optimization in internal coordinates. *Proteins*, (suppl. 1), 215–220.
28. Datto,M.B. *et al*. (1995) Functional analysis of the transforming growth factor beta responsive elements in the WAF1/Cip1/p21 promoter. *J. Biol. Chem.*, **270**, 28623–28628.
29. Vannini,A. *et al*. (2004) Crystal structure of a eukaryotic zinc-dependent histone deacetylase, human HDAC8, complexed with a hydroxamic acid inhibitor. *Proc. Natl Acad. Sci. USA*, **101**, 15064–15069.
30. Rocchi,P. *et al*. (2005) p21Waf1/Cip1 is a common target induced by short-chain fatty acid HDAC inhibitors (valproic acid, tributyrin and sodium butyrate) in neuroblastoma cells. *Oncol. Rep.*, **13**, 1139–1144.
31. Nian,H. *et al*. (2009) Modulation of histone deacetylase activity by dietary isothiocyanates and allyl sulfides: studies with sulforaphane and garlic organosulfur compounds. *Environ. Mol. Mutagen.*, **50**, 213–221.
32. Chiba,T. *et al*. (2004) Identification of genes up-regulated by histone deacetylase inhibition with cDNA microarray and exploration of epigenetic alterations on hepatoma cells. *J. Hepatol.*, **41**, 436–445.
33. Miyanaga,A. *et al*. (2008) Antitumor activity of histone deacetylase inhibitors in non-small cell lung cancer cells: development of a molecular predictive model. *Mol. Cancer Ther.*, **7**, 1923–1930.
34. Tavares,T.S. *et al*. (2008) Gene microarray analysis of human renal cell carcinoma: the effects of HDAC inhibition and retinoid treatment. *Cancer Biol. Ther.*, **7**, 1607–1618.
35. Davis,C.D. *et al*. (2002) Selenium-enriched broccoli decreases intestinal tumorigenesis in multiple intestinal neoplasia mice. *J. Nutr.*, **132**, 307–309.
36. Finley,J.W. *et al*. (2000) Selenium from high selenium broccoli protects rats from colon cancer. *J. Nutr.*, **130**, 2384–2389.
37. Finley,J.W. *et al*. (2001) Cancer-protective properties of high-selenium broccoli. *J. Agric. Food Chem.*, **49**, 2679–2683.
38. Davis,C.D. *et al*. (1999) The chemical form of selenium influences 3,2′-dimethyl-4-aminobiphenyl-DNA adduct formation in rat colon. *J. Nutr.*, **129**, 63–69.
39. Feng,Y. *et al*. (1999) Dietary selenium reduces the formation of aberrant crypts in rats administered 3,2′-dimethyl-4-aminobiphenyl. *Toxicol. Appl. Pharmacol.*, **157**, 36–42.
40. Reddy,B.S. *et al*. (2000) Lack of chemopreventive efficacy of DL-selenomethionine in colon carcinogenesis. *Int. J. Mol. Med.*, **5**, 327–330.
41. Ip,C. *et al*. (2000) Chemical speciation influences comparative activity of selenium-enriched garlic and yeast in mammary cancer prevention. *J. Agric. Food Chem.*, **48**, 2062–2070.
42. Spallholz,J.E. *et al*. (2001) Dimethyldiselenide and methylseleninic acid generate superoxide in an *in vitro* chemiluminescence assay in the presence of glutathione: implications for the anticarcinogenic activity of L-selenomethionine and L-Se-methylselenocysteine.. *Nutr. Cancer*, **40**, 34–41.
43. Gopalakrishna,R. *et al*. (2001) Protein kinase C as a molecular target for cancer prevention by selenocompounds. *Nutr. Cancer*, **40**, 55–63.
44. Cooper,A.J. (2004) The role of glutamine transaminase K (GTK) in sulfur and alpha-keto acid metabolism in the brain, and in the possible bioactivation of neurotoxicants. *Neurochem. Int.*, **44**, 557–577.
45. Lee,J. *et al*. (2009) α-Keto acid metabolites of naturally-occurring organoselenium compounds as inhibitors of histone deacetylase in human prostate cancer cells. *Cancer Prev. Res.* in press.
46. Lippman,S.M. *et al*. (2009) Effect of selenium and vitamin E on risk of prostate cancer and other cancers: the Selenium and Vitamin E Cancer Prevention Trial (SELECT). *JAMA*, **301**, 39–51.

Received March 13, 2009; revised June 8, 2009; accepted June 9, 2009